

# Stabilizing an individual charge fluctuator in a Si/SiGe quantum dot

Feiyang Ye,<sup>1,\*</sup> Ammar Ellaboudy,<sup>1,\*</sup> and John M. Nichol<sup>1,†</sup>

<sup>1</sup>*Department of Physics and Astronomy, University of Rochester, Rochester, NY, 14627 USA*

Charge noise is a major obstacle to improved gate fidelities in silicon spin qubits. Numerous methods exist to mitigate charge noise, including improving device fabrication, dynamical decoupling, and real-time parameter estimation. In this work, we demonstrate a new class of techniques to mitigate charge noise in semiconductor quantum dots by controlling the noise sources themselves. Using two different classical feedback methods, we stabilize an individual charged two-level fluctuator in a Si/SiGe quantum dot. These control methods reduce the low-frequency component of the noise power spectrum by an order of magnitude. These techniques also enable stabilizing the fluctuator in either of its states. In the future, such techniques may enable improved coherence times in quantum-dot spin qubits.

## INTRODUCTION

Spin qubits based on gate-defined semiconductor quantum dots are excellent qubits due to their long coherence times, small size, and compatibility with advanced semiconductor manufacturing techniques [1]. Most gate-defined quantum dots rely on precise control of the electrostatic confinement potential to achieve initialization, readout, as well as single- and multi-qubit gates. Thus, random electrical noise in the device that disturbs the confinement potentials, or charge noise, is a major obstacle in improving spin qubit fidelity. While not completely understood, the microscopic description of charge noise likely involves an ensemble of two-level fluctuators (TLFs) in the host material, which result in a  $1/f$ -like noise power spectrum [1–15].

Potential options for mitigating charge noise involve design choices including the width [14] or depth [10] of the quantum well, the morphology of any capping layers [14], or the thickness of the gate dielectric [6]. Dynamical-decoupling protocols can filter the low-frequency noise of the environment, increasing the coherence time of the qubit [4, 13, 16, 17]. Real-time feedback of sensor [18] or qubit [19, 20] parameters can also reduce the effect of charge fluctuations. Another promising technique involves stabilizing the fluctuators themselves. This strategy has been applied effectively in the case of hyperfine fluctuations in spin-qubit systems [21, 22]. The possibility of coherent control of electrically active two-level systems has been established in superconducting quantum systems [23]. Additionally, two-level systems, just like qubits, can also be dynamically decoupled through a variety of mechanisms [24, 25].

In this work, we report two feedback methods to stabilize an electrically active TLF in a Si/SiGe quantum dot. Both techniques leverage the sensitive voltage dependence of the TLF switching times in quantum dots [15], and both methods involve monitoring the state of the TLF in real time. When the TLF switches its state, we change the gate voltages to a configuration where the TLF switching time decreases. In the first open-loop

method, we wait a fixed amount of time at this fast tuning, before returning to the original slow tuning. In the second closed-loop method, we monitor the TLF state in the fast tuning and return to the slow tuning after it has switched back to the desired state. Both methods reduce the low-frequency fluctuations of the TLF by nearly an order of magnitude. We also demonstrate that feedback can be used to stabilize the TLF in either of its states, and the performance of both agrees with numerical simulations. In the future, these methods could be used to suppress charge noise in spin-qubit devices, improving their coherence times.

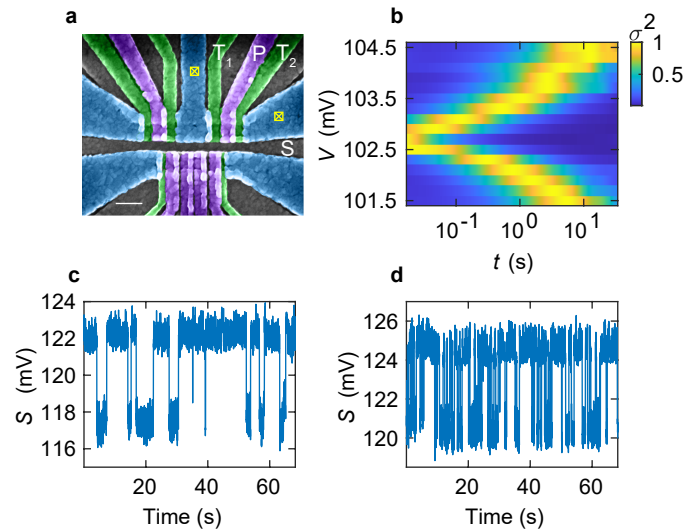


FIG. 1. **Experimental setup.** **a** The experiments reported here use the upper right quantum dot in a multi-dot device. **b** Normalized Allan variance of the TLF signal at different gate voltages  $V$  applied to the screening gate  $S$ . For each value of  $V$ , we also adjust the plunger-gate voltage to keep the quantum-dot chemical potential fixed. The TLF switching time depends sensitively on gate voltages. **c** Example time series for the slow tuning. **d** Example time series for the fast tuning.

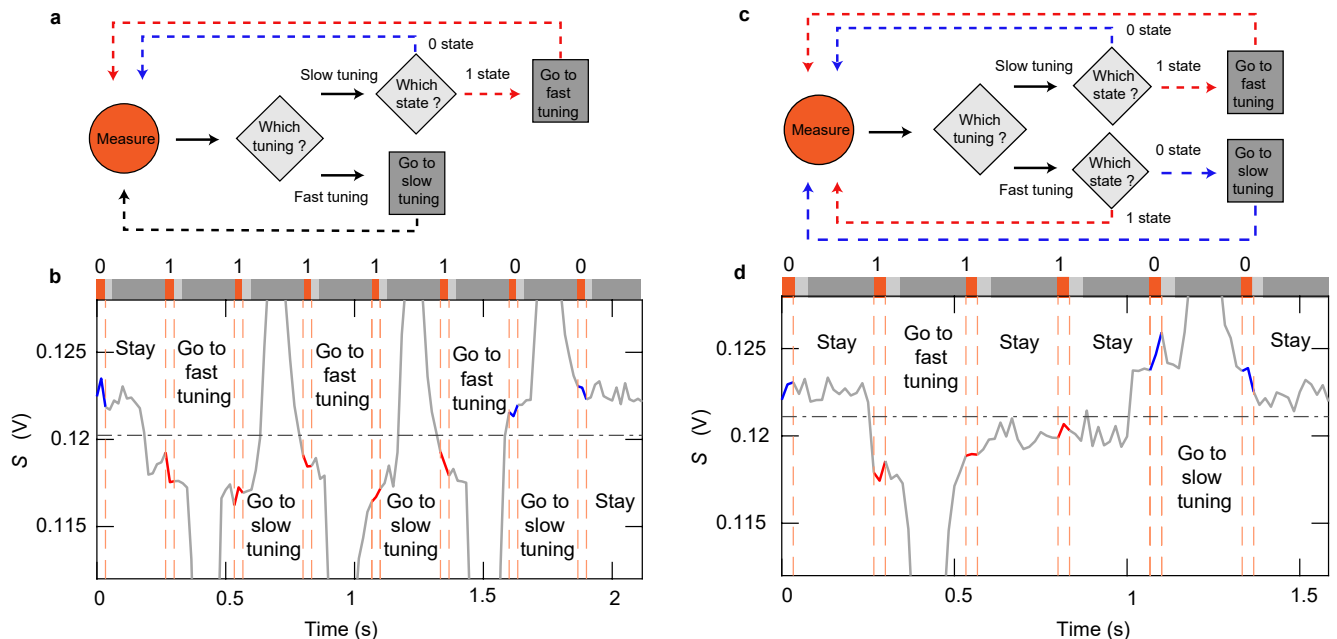


FIG. 2. **Feedback methods.** **a** In the open-loop control method, we monitor the TLF state in the slow tuning. If the TLF is measured in the 1 state, we change to the fast tuning for a set amount of time, and then return to the slow tuning. **b** Actual time series recorded during the open-loop process, with decisions indicated. The gray trace is the actual measured signal. The large deviations in the signal are the result of the voltage pulses during the tuning change. The colored segments indicate the state of the TLF determined during each measurement segment, where the signal threshold is indicated by the horizontal dashed line. **c** In the closed-loop control method, we also monitor the state of the TLF in the fast tuning, and we return to the slow tuning once the TLF is found in the 0 state. **d** Actual time series recorded during the closed-loop process, with decisions indicated.

## EXPERIMENTAL SETUP

The experiments described here involve a single quantum dot in a Si/SiGe heterostructure with an 8-nm-wide quantum well 50 nm below the surface of the semiconductor (Fig. 1a). The device is fabricated with an overlapping gate architecture and is configured for radiofrequency reflectometry [26]. We operate the device at a temperature of 10 mK in a dilution refrigerator. The other dots in the device are either tuned deep in the Coulomb blockade regime or the accumulation regime with many electrons.

We tune the quantum dot to the Coulomb blockade regime and fix its chemical potential on the side of a transport peak, where the conductivity of the dot is maximally sensitive to chemical potential fluctuations. We measure changes in the dot conductance via radiofrequency reflectometry. As reported previously, we find pronounced random telegraph noise, with the TLF switching between two states, which we label as “0” and “1”. Based on measurements of the TLF occupation probability, we identify the 0 state as the ground state. Moreover, we observe that the characteristic switching time depends sensitively on gate voltages [15] (Fig. 1b).

In the remainder of this work, we will use two different

voltage settings, or tunings, which feature different TLF switching times. We refer to the first as the “slow tuning,” where the switching time is on the order of seconds or slower (Fig. 1c). We also use a “fast tuning,” where the switching time is of order seconds or faster (Fig. 1d). These two tunings differ by voltages applied to both the plunger gate and screening gate (Fig. 1b), such that the chemical potential of the quantum dot is approximately the same in both tunings [15]. In the following, we will refer to the mean time spent in the 0 state before a transition to the 1 state in the fast (slow) tunings as  $\tau_0^{fast}$  ( $\tau_0^{slow}$ ). Likewise, we will denote the mean time spent in the 1 state before a switch to the 0 state as  $\tau_1^{fast}$  ( $\tau_1^{slow}$ ). For most of the experiments described below, we will stabilize the TLF in the 0 state. Thus, we will expect  $\tau_1^{slow}$  to decrease with feedback, as the TLF spends less time in its excited state.

## OPEN-LOOP CONTROL

The primary idea of our open-loop feedback method is that the switching times of the TLF decrease significantly in the fast tuning, compared to the slow tuning. If we wish to stabilize the TLF in the 0 state, and if we find

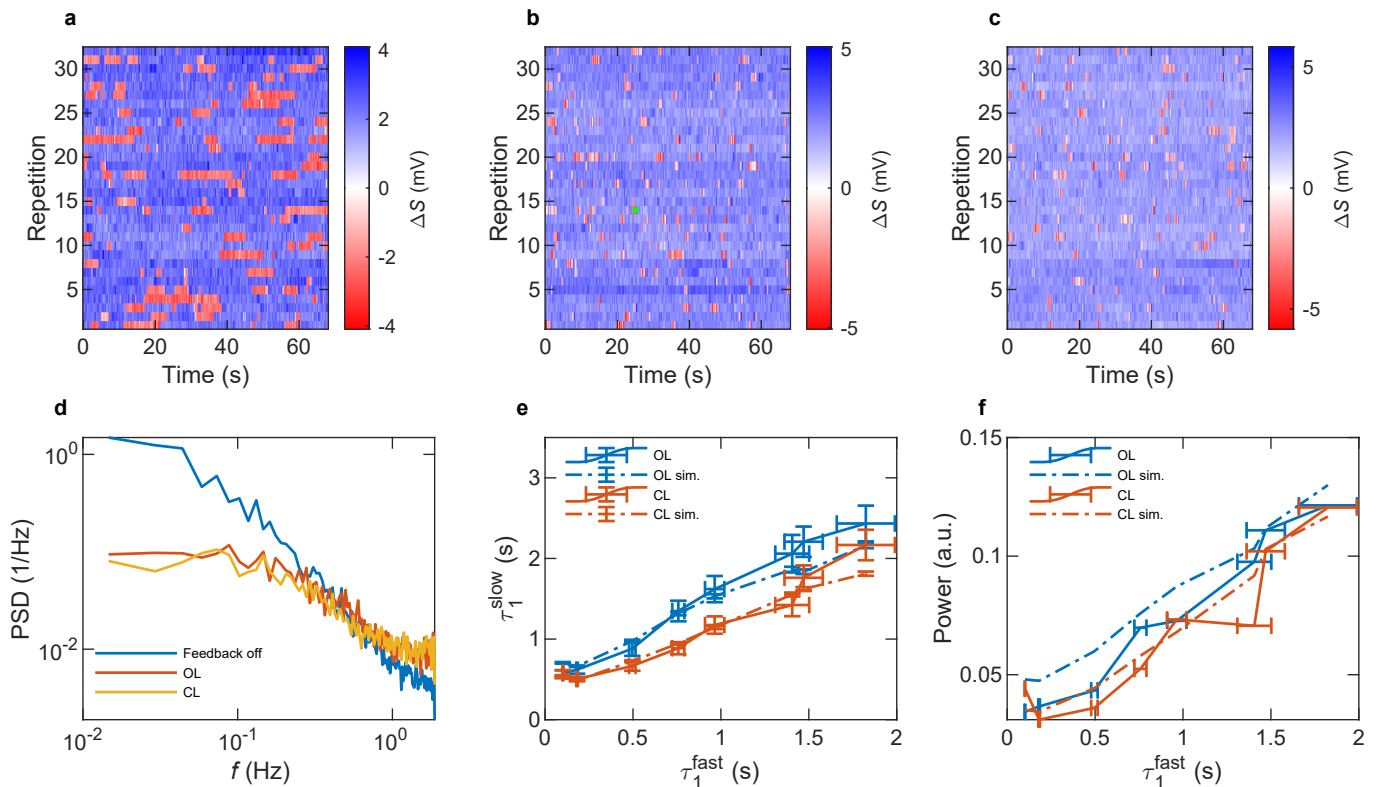


FIG. 3. **Stabilizing the TLF in 0 state.** **a** Representative measurements of the TLF without any feedback. The vertical axis represents different repetitions. The blue color corresponds to the 0 state, and the red color corresponds to the 1 state. The colorbar  $\Delta S$  shows the difference between the measured signal and the threshold. **b** and **c** show measurements of the same TLF with open-loop (OL) and closed-loop (CL) feedback, respectively. The green point in **b** marks an error in our readout, because the gate-voltage change overlaps with the readout window. **d** The power spectra of the clustered signals for the 3 cases show that the low-frequency noise reduces by an order of magnitude after applying feedback. **e** Measured and simulated mean time spent in the 1 state for different fast-tuning switching times. As  $\tau_1^{fast}$  decreases, the feedback performs better, and the TLF spends less time in the 1 state. **f** Integrated power from 0 to 1 Hz for the different feedback methods, and simulations.

it to be in the 1 state in the slow tuning, we can significantly increase the probability of finding it back in the 0 state by waiting for a time on the order of  $\tau_1^{fast} \ll \tau_1^{slow}$  in the fast tuning. In this procedure, we divide the total feedback cycle, which takes  $\Delta T = 8/30$  s, into two parts: measurement and feedback (Figs. 2a-b). The measurement segment takes  $\Delta T/8$ . We use the reflectometry signal acquired during this time to determine the TLF state. In the feedback segment, which lasts  $7\Delta T/8$ , we change the gate voltages if required. Specifically, if we find the TLF in the 1 state during the measurement window, we change to the fast tuning and then return to the slow tuning during the next feedback segment. Due to the low-pass filters installed in our setup, the time to change the gate voltages occupies a significant fraction of  $7\Delta T/8$  and takes a few hundred milliseconds (Fig. 2b). If, during the measurement window, we find the TLF in the 0 state, we do not change the tuning. After the feedback segment, the entire cycle repeats. In these experiments, the length of the feedback cycle is primarily constrained by the length of time it takes to change the gate voltages.

As discussed further below, significant improvements can be made to this setup to increase its speed.

Figure 3a shows representative time-series data for the TLF we measure without any feedback. Figure 3b shows time-series data for the same TLF with open-loop feedback. Visual inspection confirms effective stabilization of the 0 state. To assess the performance of this method, we perform 32 repetitions of 256 feedback cycles, acquiring a time series of length  $256 \times \Delta T \approx 68$  s for each repetition. To avoid errors in our state assignment due to drifts in the tuning, we update the 0/1 signal threshold every four repetitions. To quantify the performance of the feedback, we threshold the resulting time series data using a Gaussian Mixture Model to determine the state of the TLF as a function of time. We take the power spectrum of the resulting time series for the case with no feedback and the case with feedback, and we compare them in Fig. 3d. For frequencies below about  $1/\tau_1^{fast} \approx 1$  Hz, the power spectral density of fluctuations associated with this TLF decreases by more than an order of magnitude.

We also investigate the performance of this method as

we change  $\tau_1^{fast}$ . As expected, the measured values of  $\tau_1^{slow}$  increase with  $\tau_1^{fast}$ , reflecting the decreased performance of the feedback process as the switching times in the fast tuning increase, as expected (Fig. 3e). Figure 3f plots the integrated power spectral density of the TLF time series from 0 to 1 Hz, and this value also shows a corresponding increase, reflecting diminished performance of the feedback loop as  $\tau_1^{fast}$  increases.

Figures 3e and f also show the results of our numerical simulations, which agree quantitatively with the experimental data. In these simulations, we treat the TLF as a classical random telegraph fluctuator, and we model transitions as a continuous-time Markov process. We calculate the transition probability at each time step using the Kolmogorov backward equations  $\frac{dP(t)}{dt} = QP(t)$  where  $Q$  is the transition rate matrix [27]. We calculate the transition rate matrix using transition rates extracted from the experiment without feedback. We estimate the transition rates from the mean switching time  $\tau$  of each state where  $\Gamma_{1/0} = 1/\tau_{1/0}$ . We simulate the two methods with time step  $\Delta T$  and with 256 feedback cycles. The simulation results shown in Figs. 3e and f are the average of 1000 repetitions. In all cases, the simulations agree quantitatively with our results.

## CLOSED-LOOP CONTROL

The closed-loop feedback method is similar to open-loop method, except that we monitor the state of the TLF in the fast tuning, and we return to the slow tuning only when the TLF has switched back to the desired state (Figs. 2c,d). As before, we stabilize the TLF in the 0 state in the slow tuning. Figure 3c shows the time series of the TLF signal when the feedback is applied. Comparing with Fig. 3a again shows significantly reduced time in the 1 state. Figures 3d-f illustrate the performance of closed-loop method. As expected, it performs better than the open-loop method because we actively monitor the state of the TLF in the fast tuning. As before, our results agree with the simulations.

To demonstrate the utility of the closed-loop method, we also stabilize the TLF in its excited state (the 1 state). Figures 4a and b show the time series data for the cases with the feedback off and on, respectively. With the feedback applied, we find that  $\tau_0^{slow}$  decreases as  $\tau_0^{fast}$  decreases, reflecting the effect of the feedback. As  $\tau_0^{slow}$  decreases (Fig. 4d), the TLF spends more time in its excited state (Fig. 4c). As before, our results agree with our numerical simulations. These results highlight the flexibility of this technique to stabilize electrical TLFs in either of their states.

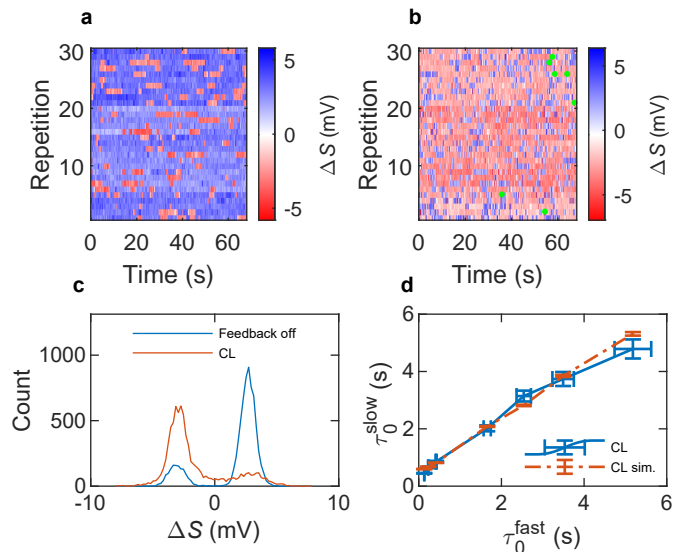


FIG. 4. **Stabilizing the TLF in 1 state.** **a** Time series while feedback is off. **b** Time series while closed-loop feedback is on. **c** Histogram of sample time series with feedback on and off. **d** As  $\tau_0^{fast}$  increases, the feedback performs less effectively, and  $\tau_0^{slow}$  increases.

## CONCLUSION

Low-frequency charge noise is a major challenge affecting spin qubit gate fidelities. In this work, we have demonstrated a class of techniques that mitigate charge noise by directly controlling the sources of noise themselves. A number of improvements could be made to our setup to increase its effectiveness. The longest elements of our feedback cycle, which currently lasts 267 ms, involve data transfer between the data acquisition card and our software, and the voltage pulses, which pass through low-pass filters. Instead, with a field-programmable gate array and wiring compatible with fast voltage pulses, the cycle time could likely be reduced to the millisecond level or below, significantly increasing the bandwidth of our techniques.

Recent theoretical work has shown that individual TLFs can indeed have a significant impact on qubit performance [28], and that removing such fluctuators can enhance qubit coherence. Thus, the techniques we have discussed to stabilize individual TLFs may help to improve spin-qubit coherence. Applying our techniques to spin qubits will depend critically on the ability to resolve individual voltage-dependent TLFs in real time in spin-qubit devices. In prior work, we have found that TLFs in our devices frequently appear to depend on gate voltages [15]. Recent work has also demonstrated the possibility of real-time measurements of charge noise in spin qubits [20]. While not all TLFs will have a large enough effect to enable rapid real-time measurement, those TLFs that are large enough for real-time measure-

ment will likely have the most significant effects on spin qubit performance and will thus be the most important to stabilize. It could also be that advanced signal processing techniques, such as hidden Markov modeling [29], could be used to distinguish the states of TLFs where simple threshold techniques do not suffice.

### ACKNOWLEDGMENTS

This work was sponsored by the Army Research Office through Grant No. W911NF-23-1-0115 and the Air Force Office of Scientific Research through Grant No. FA9550-23-1-0710. The views and conclusions contained in this document are those of the authors and should not be interpreted as representing the official policies, either expressed or implied, of the Army Research Office or the U.S. Government. The U.S. Government is authorized to reproduce and distribute reprints for Government purposes notwithstanding any copyright notation herein.

### AUTHOR CONTRIBUTIONS

F.Y., A.E., and J.M.N. formulated the experiment and carried out the measurements; all authors wrote the paper; J.M.N. supervised the research.

---

\* These authors contributed equally.

† [john.nichol@rochester.edu](mailto:john.nichol@rochester.edu)

- [1] G. Burkard, T. D. Ladd, A. Pan, J. M. Nichol, and J. R. Petta, Semiconductor spin qubits, *Rev. Mod. Phys.* **95**, 025003 (2023).
- [2] E. Paladino, Y. M. Galperin, G. Falci, and B. L. Altshuler,  $1/f$  noise: Implications for solid-state quantum information, *Rev. Mod. Phys.* **86**, 361 (2014).
- [3] B. M. Freeman, J. S. Schoenfield, and H. Jiang, Comparison of low frequency charge noise in identically patterned Si/SiO<sub>2</sub> and Si/SiGe quantum dots, *Appl. Phys. Lett.* **108**, 253108 (2016).
- [4] J. Yoneda, K. Takeda, T. Otsuka, T. Nakajima, M. R. Delbecq, G. Allison, T. Honda, T. Kodera, S. Oda, Y. Hoshi, N. Usami, K. M. Itoh, and S. Tarucha, A quantum-dot spin qubit with coherence limited by charge noise and fidelity higher than 99.9%, *Nature Nanotechnology* **13**, 102 (2018).
- [5] X. Mi, S. Kohler, and J. R. Petta, Landau-Zener interferometry of valley-orbit states in Si/SiGe double quantum dots, *Phys. Rev. B* **98**, 161404 (2018).
- [6] E. J. Connors, J. Nelson, H. Qiao, L. F. Edge, and J. M. Nichol, Low-frequency charge noise in Si/SiGe quantum dots, *Phys. Rev. B* **100**, 165305 (2019).
- [7] T. Struck, A. Hollmann, F. Schauer, O. Fedorets, A. Schmidbauer, K. Sawano, H. Riemann, N. V. Abrosimov, Ł. Cywiński, D. Bougeard, *et al.*, Low-frequency spin qubit energy splitting noise in highly purified 28si/sige, *npj Quantum Information* **6**, 40 (2020).
- [8] L. Petit, J. Boter, H. Eenink, G. Droulers, M. Tagliaferri, R. Li, D. Franke, K. Singh, J. Clarke, R. Schouten, V. Dobrovitski, L. Vandersypen, and M. Veldhorst, Spin Lifetime and Charge Noise in Hot Silicon Quantum Dot Qubits, *Phys. Rev. Lett.* **121**, 076801 (2018).
- [9] M. Rudolph, B. Sarabi, R. Murray, M. Carroll, and N. M. Zimmerman, Long-term drift of si-mos quantum dots with intentional donor implants, *Scientific Reports* **9**, 7656 (2019).
- [10] L. Kranz, S. K. Gorman, B. Thorgrimsson, Y. He, D. Keith, J. G. Keizer, and M. Y. Simmons, Exploiting a single-crystal environment to minimize the charge noise on qubits in silicon, *Adv. Mater.* **32**, 2003361 (2020).
- [11] A. Elsayed, M. Shehata, C. Godfrin, S. Kubicek, S. Massar, Y. Canvel, J. Jussot, G. Simion, M. Mongillo, D. Wan, *et al.*, Low charge noise quantum dots with industrial cmos manufacturing, *arXiv preprint arXiv:2212.06464* (2022).
- [12] N. Holman, D. Rosenberg, D. Yost, J. Yoder, R. Das, W. D. Oliver, R. McDermott, and M. Eriksson, 3d integration and measurement of a semiconductor double quantum dot with a high-impedance tin resonator, *npj Quantum Information* **7**, 137 (2021).
- [13] E. J. Connors, J. Nelson, L. F. Edge, and J. M. Nichol, Charge-noise spectroscopy of Si/SiGe quantum dots via dynamically-decoupled exchange oscillations, *Nat. Commun.* **13**, 940 (2022).
- [14] B. Paquelet Wuetz, D. Degli Esposti, A.-M. J. Zwerver, S. V. Amitonov, M. Botifoll, J. Arbiol, L. M. Vandersypen, M. Russ, and G. Scappucci, Reducing charge noise in quantum dots by using thin silicon quantum wells, *Nat. Commun.* **14**, 1385 (2023).
- [15] F. Ye, A. Ellaboudy, D. Albrecht, R. Vudatha, N. T. Jacobson, and J. M. Nichol, Characterization of individual charge fluctuators in si/sige quantum dots (2024), *arXiv:2401.14541 [cond-mat.mes-hall]*.
- [16] J. Medford, L. Cywiński, C. Barthel, C. M. Marcus, M. P. Hanson, and A. C. Gossard, Scaling of dynamical decoupling for spin qubits, *Phys. Rev. Lett.* **108**, 086802 (2012).
- [17] J. Bylander, S. Gustavsson, F. Yan, F. Yoshihara, K. Harrabi, G. Fitch, D. G. Cory, Y. Nakamura, J.-S. Tsai, and W. D. Oliver, Noise spectroscopy through dynamical decoupling with a superconducting flux qubit, *Nature Physics* **7**, 565 (2011).
- [18] T. Nakajima, Y. Kojima, Y. Uehara, A. Noiri, K. Takeda, T. Kobayashi, and S. Tarucha, Real-time feedback control of charge sensing for quantum dot qubits, *Physical Review Applied* **15**, L031003 (2021).
- [19] M. D. Shulman, S. P. Harvey, J. M. Nichol, S. D. Bartlett, A. C. Doherty, V. Umansky, and A. Yacoby, Suppressing qubit dephasing using real-time hamiltonian estimation, *Nature Communications* **5**, 5156 (2014).
- [20] J. Park, H. Jang, H. Sohn, J. Yun, Y. Song, B. Kang, L. E. Stehouwer, D. D. Esposti, G. Scappucci, and D. Kim, Passive and active suppression of transduced noise in silicon spin qubits (2024), *arXiv:2403.02666*.
- [21] H. Bluhm, S. Foletti, D. Mahalu, V. Umansky, and A. Yacoby, Enhancing the Coherence of a Spin Qubit by Operating it as a Feedback Loop That Controls its Nuclear Spin Bath, *Phys. Rev. Lett.* **105**, 216803 (2010).
- [22] J. M. Nichol, L. A. Orona, S. P. Harvey, S. Fallahi, G. C. Gardner, M. J. Manfra, and A. Yacoby, High-fidelity entangling gate for double-quantum-dot spin qubits, *npj*

- [Quant. Info. 3, 3 \(2017\)](#).
- [23] J. Lisenfeld, C. Müller, J. H. Cole, P. Bushev, A. Lukashenko, A. Shnirman, and A. V. Ustinov, Measuring the temperature dependence of individual two-level systems by direct coherent control, [Physical Review Letters 105, 230504 \(2010\)](#).
  - [24] S. Matityahu, H. Schmidt, A. Bilmes, A. Shnirman, G. Weiss, A. V. Ustinov, M. Schechter, and J. Lisenfeld, Dynamical decoupling of quantum two-level systems by coherent multiple Landau–Zener transitions, [npj Quantum Inf. 5, 114 \(2019\)](#).
  - [25] D. Niepce, J. J. Burnett, M. Kudra, J. H. Cole, and J. Bylander, Stability of superconducting resonators: Motional narrowing and the role of Landau-Zener driving of two-level defects, [Science Advances 7, eabh0462 \(2021\)](#).
  - [26] E. J. Connors, J. Nelson, and J. M. Nichol, Rapid high-fidelity spin-state readout in Si/Si-Ge quantum dots via rf reflectometry, [Phys. Rev. Applied 13, 024019 \(2020\)](#).
  - [27] J. R. Norris, *Markov Chains* (Cambridge University Press, Cambridge, UK, 1997).
  - [28] M. Mehmandoost and V. Dobrovitski, Decoherence induced by a sparse bath of two-level fluctuators: peculiar features of  $1/f$  noise in high-quality qubits (2024), [arXiv:2404.18659](#).
  - [29] D. Albrecht and N. T. Jacobson, NoMoPy: Noise Modeling in Python (2023), [arXiv:2311.00084 \[stat.CO\]](#).